communications physics

ARTICLE

https://doi.org/10.1038/s42005-023-01252-7 OPEN

Action of the general anaesthetic isoflurane reveals coupling between viscoelasticity and electrophysiological activity in individual neurons

Casey Adam[1,2]✉, Celine Kayal[1,2], Ari Ercole[3], Sonia Contera[4]✉, Hua Ye[1,2] & Antoine Jerusalem[1]✉

General anaesthetics are widely used for their analgesic, immobilising, and hypnotic effects. The mechanisms underlying these effects remain unclear, but likely arise from alterations to cell microstructure, and potentially mechanics. Here we investigate this hypothesis using a custom experimental setup combining calcium imaging and nanoindentation to quantify the firing activity and mechanical properties of dorsal root ganglion-derived neurons exposed to a clinical concentration of 1% isoflurane gas, a halogenated ether commonly used in general anaesthesia. We found that cell viscoelasticity and functional activity are simultaneously and dynamically altered by isoflurane at different stages of exposure. Particularly, cell firing count correlated linearly with the neuronal loss tangent, the ratio of mechanical energy dissipation and storage by the cell. Our results demonstrate that anaesthetics affect cells as a whole, reconciling seemingly contradictory theories of how anaesthetics operate, and highlight the importance of considering cell mechanics in neuronal functions, anaesthesia, and clinical neuroscience in general.

[1] Department of Engineering Science, University of Oxford, Parks Road, Oxford OX1 3PJ, UK. [2] Institute of Biomedical Engineering, University of Oxford, Old Road Campus, Roosevelt Drive, Oxford OX3 7DQ, UK. [3] Division of Anaesthesia, University of Cambridge, Addenbrooke's Hospital, Cambridge CB2 0QQ, UK. [4] Department of Physics, University of Oxford, Parks Road, Oxford OX1 3PU, UK. ✉email: adamc@purdue.edu; sonia.antoranzcontera@physics.ox.ac.uk; antoine.jerusalem@eng.ox.ac.uk

General anaesthetics play a crucial role in medicine and physiology[1,2]. Most modern medical procedures are rendered possible via the hypnotic, amnesic and analgesic effects of general anaesthetics[1,2]. Anaesthetics affect all life forms[1], and are produced naturally during physiological stress responses[1]. In spite of the prevalent use and universal effects of general anaesthetics, the mechanisms by which anaesthetics operate remain incompletely understood.

Historically, anaesthetics have been hypothesised to operate by interacting either with the membrane's lipid bilayer, or with proteins such as ion channels[3]. Often, both theories are presented in opposition, despite indications that they are not mutually exclusive[1,4–7]. While it is known that general anaesthetics act upon a wide variety of membrane receptors and channels[7], this fact does not invalidate previous observations that general anaesthetics also affect other subcellular structures[1,3]. For example, general anaesthetics modulate cytoskeletal dynamics[1,4]. Actin and spectrin, prevalent components of neuronal cytoskeletons, are affected by general anaesthetics[5]. Alterations to cytoskeleton dynamics by general anaesthetics in turn affect cell contractile activity[6] as well as the spatial arrangement of proteins in the cell membrane[1,7]. Additionally, general anaesthetics fluidise lipid membranes[5,8] and alter lipid raft formation[7], thereby altering the properties of the cell membrane, lipids and constituent proteins, as a whole[1,3,9]. These effects are potentially due to alterations in the charge distribution and hence intermolecular interactions between subcellular components of the neuron when general anaesthetics are present[10,11]. Therefore, general anaesthetics likely have pleiotropic effects on cells[1,3].

Ultimately, changes induced by general anaesthetics alter the electrophysiological properties of the brain[12,13]. For instance, electroencephalography (EEG) studies show altered brain activity patterns in patients under anaesthesia[12,13], thus suggesting that general anaesthetics alter action potential generation and propagation by individual neurons. While action potential propagation is traditionally viewed in terms of cell electrophysiology[14], action potentials are also characterised by mechanical, chemical, pH and heat changes that couple with the voltage changes[3]. In other words, action potentials are not solely electrical in nature, but exhibit complex coupling between properties underpinned by nonequilibrium thermodynamics[3,15,16]. The mechanical component of action potentials is of particular interest, since mechanical properties arise from intermolecular interactions[17]. However, new experimental frameworks are needed to establish and quantify whether general anaesthetics induce electrophysiological and mechanical changes in individual neurons, and whether these changes concurrently and/or collaboratively occur.

To this end, a custom experimental apparatus[18–20], shown in Fig. 1a, was created by mounting a nanoindenter on an inverted microscope enclosed in a sealed tubular flow system. Neurons inside this apparatus were exposed to one of three treatments: flowing 1% isoflurane gas, a halogenated ether commonly used as an inhalational anaesthetic[2], flowing air as a control for the effects of isoflurane, or no flow as a control to distinguish the effects of gas flow from those of the gas itself. To quantify how each treatment affected cells through time, measurements were performed at six specific time points: Before, 15 min During, 30 min During, 45 min During, 30 min After and 45 min After exposure to each treatment, as shown in Fig. 1(b). Calcium imaging (detailed in Supplementary Figures S1, S3 and S4) was used to measure cell firing, or microscale dynamic mechanical analysis (DMA, detailed in Supplementary Figures S1 and S2) at different frequencies was used to measure whole-cell (membrane, mostly cytoskeleton and possibly nucleus[21]) viscoelasticity. Using this setup, we show that isoflurane alters both the mechanical properties and firing activity of individual neurons, and that these alterations correlate linearly with one another. These findings reconcile the different theories proposed to explain the mechanism of general anaesthesia by demonstrating that the cellular mechanical structure as a whole is linked to functional alterations during anaesthetic exposure. They also have wider implications on the role of mechanics in electrophysiology by demonstrating that action potentials are defined and controlled by the collaborative and concurrent effect of cell mechanics in what has traditionally been viewed as a purely bioelectrical phenomenon.

Results and discussion

Effect of isoflurane on neuron firing. Calcium imaging was used to record the functional activity of each neuron within the microscope's field of view. The fraction of the cell population that fired and the mean number of firing events were calculated from functional activity measurements in order to determine isoflurane's effects on neuron firing. Figure 2a shows how the fraction of neurons that fire, n_f — calculated as the number of cells that fired at a specific time point divided by the total number of cells in the microscope's field of view — varied with each treatment and experimental time point (for the purpose of firing count, a time point is defined as a 3 min window captured at a 400 ms frame rate). Cells subjected to gas flow (isoflurane or air) fired significantly less than no flow control cells ($p < 0.04$, Wilcoxon rank-sum test, individual p-values and test details can be found in Supplementary Table S2). Therefore, gas flow through the system reduces n_f. Also shown in Supplementary Table S2, n_f was similar at almost all experimental time points for cells subjected to isoflurane and flowing air. However, significantly ($p = 0.03$, Wilcoxon rank-sum test, details in Supplementary Table S2) fewer neurons exposed to isoflurane for 30 min fired compared to those exposed to flowing air for 30 min.

Figure 2b shows how the mean number of firing events, c_f, varied with each experimental treatment and time point. Histograms of c_f can be found in Supplementary Fig. S5. In the last two experimental time points (30 and 45 min After), no flow control cells fired significantly more than cells subjected to isoflurane or flowing air ($p \leq 0.014$, Wilcoxon rank-sum test, individual p-values and test details can be found in Supplementary Table S3). Therefore, gas flow reduces cell firing at the end of the experiment. Also detailed in Supplementary Table S3, neurons exposed to isoflurane for 30 min fired significantly fewer times than those exposed to flowing air ($p \leq 0.004$, Wilcoxon rank-sum test, individual p-values and test details can be found in Supplementary Table S3). The mean number of firing events did not vary significantly between neurons exposed to isoflurane and air for 45 min (individual p-values and test details can be found in Supplementary Table S3).

Figure 2 shows that neuron firing in response to isoflurane is time dependent. Since there was only 1% isoflurane flowing into the box, and since the box volume is much larger than that of a petri dish, it likely required more than 15 min for the isoflurane to diffuse into the cells. The fact that n_f and c_f did not significantly differ between isoflurane and air after 15 min of exposure supports the notion that the isoflurane was still diffusing into the cells at this time point, and hence had yet to affect the neurons. The fact that n_f and c_f significantly decreased at 30 min of isoflurane exposure compared to air suggests that cells initially respond to isoflurane by deactivating. Since n_f and c_f did not significantly differ between isoflurane and air at 45 min of exposure, it is likely that cells either compensated for the presence of isoflurane, or that a subpopulation of neurons activated in response to prolonged isoflurane exposure.

Supplementary Table S4 shows p-values describing how c_f changed with each time point. For all treatments, c_f significantly ($p \leq 0.02$, Wilcoxon rank sum test, details and individual p-values in

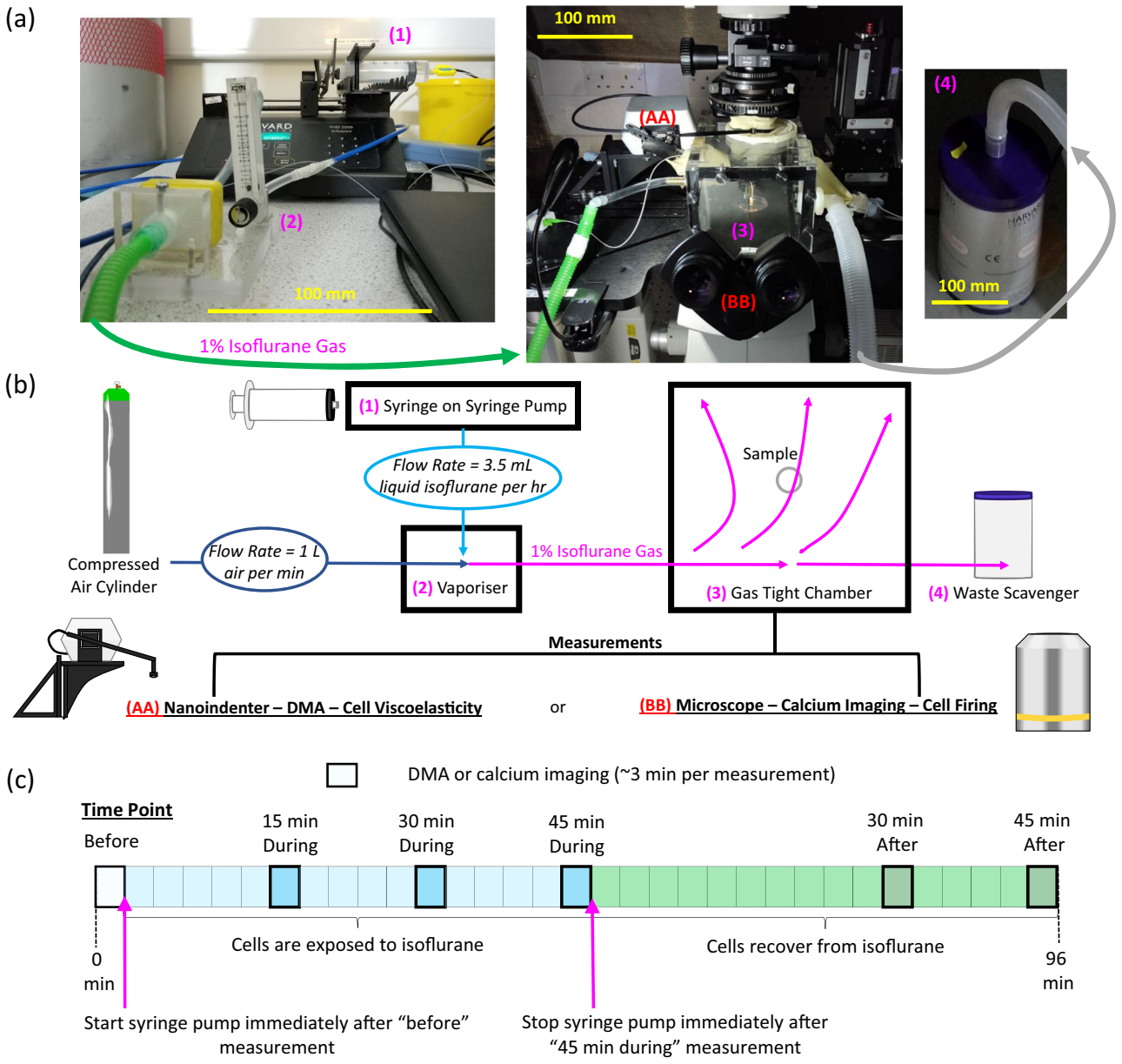

Fig. 1 Custom experimental apparatus. Panel (**a**) shows the apparatus used to measure the effects of isoflurane on neuron firing and mechanics. A schematic of (**a**) is shown in (**b**). A syringe (1) filled with liquid isoflurane, or room air as a control, was secured on a syringe pump and connected to a vaporiser (2). When the pump was active, liquid isoflurane entered the vaporiser at a rate of 3.5 mL/h, vaporised, and merged with a stream of flowing air passing through the vaporiser from a compressed air cylinder (blue tubing). This mixture of isoflurane vapour and air exited the vaporiser at a rate of 1 L/min, resulting in a 1% isoflurane gas by volume, into a gas tight box containing the sample (3), then out into a waste scavenger (4). The mechanical properties of individual neurons were measured by performing dynamic mechanical analysis (DMA) via a nanoindenter (AA). Neuron firing was recorded by performing calcium imaging via an inverted microscope (BB). Measurements were performed at six experimental time points, shown in (**c**). First, measurements were performed before exposure to the gas, with an inactive syringe pump. Next, the syringe pump was activated and measurements were collected 15 min during, 30 min during and 45 min during gas exposure. Next, the pump was deactivated and measurements were performed 30 min after and 45 min after, as cells recovered. A second control, for the effects of gas flow, was performed as above, but without activating the syringe pump or opening the gas cylinder.

Supplementary Table S4) decreased between the Before measurement and the 15 min During measurement. This observation is likely due to the lack of temperature control in the apparatus, which was not possible because the temperature controller added too much noise to nanoindenter measurements. During the Before measurement, cells were likely closer to their incubation temperature of 37 °C than to room temperature (13–18 °C). From the 15 min During measurement onwards, cells had cooled to ambient temperature. Therefore, the decrease in neuron firing between these two time points is likely due to cell cooling[22,23]. This cooling might also help explain why no flow control cell n_f was consistently higher than for cells in other treatments (Fig. 2a and Supplementary Table S2). Gas flow through the system likely facilitates faster, and potentially greater, cooling.

Changes in c_f through time varied depending on the experimental treatment. For cells exposed to isoflurane, c_f decreased between the 15 and 30 min During measurements ($p = 0.01$, Wilcoxon rank-sum test, details in Supplementary Table S4), then

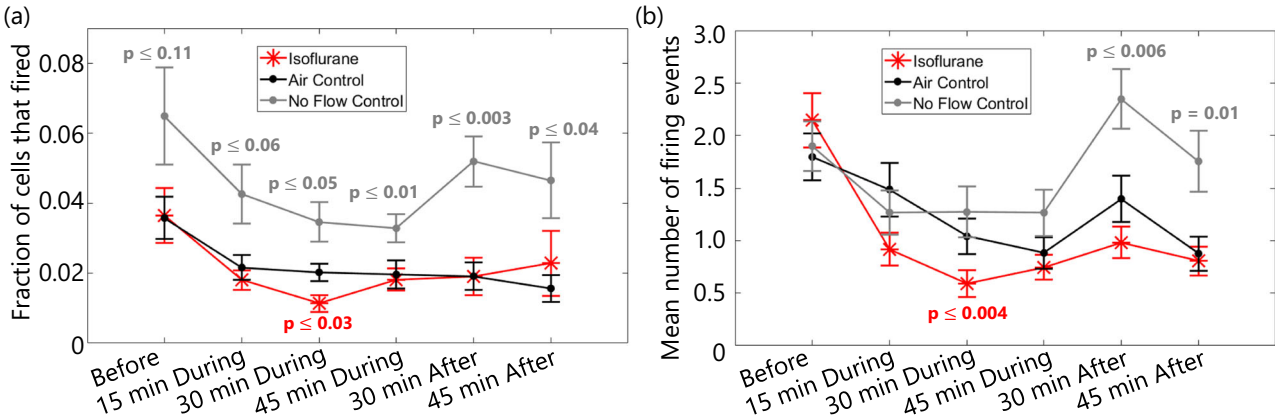

Fig. 2 Effect of isoflurane on neuron firing. The fraction of cells that fire (**a**) and the mean number of firing events (**b**) are shown for cells exposed to 1% isoflurane gas (red asterisks), flowing air (air control, black dots) or no gas flow (no flow control, grey dots) at six experimental time points: before, 15, 30 and 45 min during, and 30 and 45 min after exposure to isoflurane or flowing air. Significant differences between treatments are indicated with p values calculated from Wilcoxon rank-sum tests detailed in Supplementary Table S2 and S3 for (**a**) and (**b**), respectively. Error bars represent the standard error. Data distributions can be found in Supplementary Fig. S5.

increased between the 30 and 45 min During measurements ($p = 0.05$, Wilcoxon rank-sum test, details in Supplementary Table S4). Again, this observation suggests that neurons either compensate for the presence of isoflurane between the 30 and 45 min During measurements or that new neurons activate with longer exposure to isoflurane. Analysis of cell activation, inactivation, and reactivation was performed as detailed in the supplementary material (Supplementary Note 3, Supplementary Figs. S6 and S7 and Supplementary Tables S5–S10), to distinguish whether changes in n_f and c_f were due to cells compensating for the presence of isoflurane vs. activation of an isoflurane-specific subpopulation. Increased cell reactivation, but no change in cell (in)activation, at 45 min of exposure to isoflurane compared to both controls suggests that initially deactivated cells eventually compensate for the presence of isoflurane.

For cells exposed to flowing air, c_f did not significantly vary through time for most experimental time points (details in Supplementary Table S4). However, c_f decreased ($p = 0.04$, Wilcoxon rank-sum test, details in Supplementary Table S4) at the end of the experiment. While this change was significant only for flowing air control cells, the histograms in Supplementary Fig. S5 show that, for all three treatments, cells had a higher probability of lower firing counts at the end of the experiment. For example, the probability that $c_f = 0$ increased from 0.6 to 0.7 or 0.8 between the last two time points for cells in all three treatments. Therefore, while the only significant change occurred for flowing air, a general decrease in c_f at the end of the experiment occurred regardless of treatment. It is likely that a significant decrease in c_f would be observed for cells subjected to the isoflurane and no flow control treatments if more biological replicates were performed. Therefore, these results suggest that, in general, cells fired less at the end of the experiment, potentially because the cells have been at ambient temperature for over 90 min and start to alter their behaviour as a result.

For no flow control cells, c_f significantly increased ($p = 0.002$, Wilcoxon rank-sum test, details in Supplementary Table S4), then decreased ($p = 0.02$, Wilcoxon rank-sum test, details in Supplementary Table S4) in the last two time points. Based on the histograms in Supplementary Fig. S5, these changes in no flow control c_f were due to a few outlier cells, indicated by arrows in Supplementary Fig. S5, that increased firing at the end of the experiment. Two possibilities could explain this observation. First, the cells may belong to a sparse subpopulation of neurons with high activity. In both cases, the subpopulation would be small enough that the chances of capturing a neuron belonging to this population in the field of view are small, and hence did not occur in the isoflurane or air experiments. Second, these cells may belong to a subpopulation of neurons which are somehow activated by prolonged gas flow. In this case, the majority of the cells still behaved in a similar manner to the flowing air control. Regardless, gas flow seems to affect the fraction of cells that fire more than the number of firing events.

Effect of isoflurane on neuron mechanics. Dynamic mechanical analysis (DMA) at six different frequencies was used to measure the effects of isoflurane on neuron viscoelasticity. Figure 3 shows the storage modulus E' (Pa), loss modulus E'' (Pa) and loss tangent $\tan\delta = E''/E'$ of individual neurons at each experimental time point. To view only the mean values of E', E'' and $\tan\delta$, without individual cells included, see Supplementary Fig. S8. E', E'' and $\tan\delta$ were significantly different between experimental treatments ($p \le 0.001$, ANOVA, p-values and details in Supplementary Table S11). E' and E'' varied significantly between experimental time points ($p \le 0.02$, ANOVA, p-values and details in Supplementary Table S11). E'' and $\tan\delta$ were significantly different between measurement frequencies ($p < 0.0001$, ANOVA, individual p-values and test details in Supplementary Table S11).

Initial (Before) values of E' and E'' did not differ between treatments (Tukey's honest significant difference criterion, test details in Supplementary Table S12), and ranged within 0.1–4 kPa and 0.05–3 kPa, respectively. The large range in the data is due to cell–cell heterogeneity, and is comparable to the values previously reported in the literature[24].

Isoflurane did not significantly alter neuron mechanics when cells had only been exposed to the anaesthetic for 15 min, likely because isoflurane had yet to completely diffuse into the cells at this time point (as previously discussed). After the 30 min During time point, isoflurane significantly altered neuronal E' and E'' compared to both control treatments (Tukey's honest significant difference criterion, all p-values and test details in Supplementary Table S12). E' was significantly higher during 45 min of isoflurane exposure compared to both controls ($p = 7 \times 10^{-7}$, Tukey's honest significant difference criterion, p-values and test details in Supplementary Table S12). E'' was significantly higher for cells exposed to isoflurane both 45 min during isoflurane exposure ($p \le 0.04$, Tukey's honest significant difference criterion, p-values and test details in Supplementary Table S12) and 30 min after isoflurane

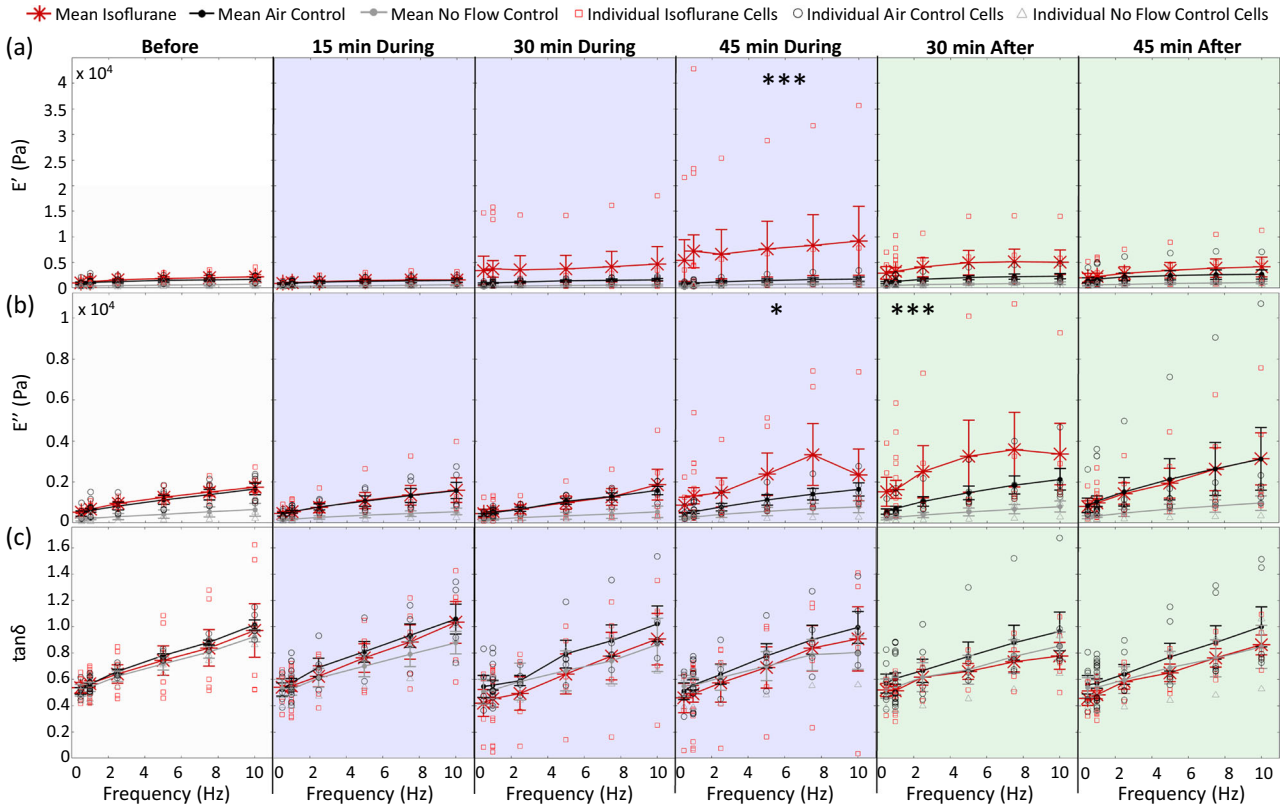

Fig. 3 Dynamic mechanical analysis of cells exposed to isoflurane. Neurons were exposed to a flow of 1% anaesthetic isoflurane gas (red asterisk), a flow of compressed air (air control, black dots), or no gas flow (no flow control, grey dots). Dynamic mechanical analysis was performed on individual cells before gas flow (Before), at 15 min intervals during gas exposure (blue shading, 15 min During, 30 min During and 45 min During), and at specific time points after gas exposure (green shading, 30 min After and 45 min After). The mean storage modulus E' (Pa), loss modulus E'' (Pa), and loss tangent $\tan\delta = E''/E'$ throughout the course of the experiment are shown in **a**–**c**, respectively. Error bars represent the standard error. Unfilled points represent individual values of: five isoflurane cells (red squares), five air control cells (black circles) and three no flow control cells (grey triangles). Significant differences between isoflurane and both control treatments, calculated by *post hoc* comparisons using Tukey's honest difference criterion (all *p*-values and test details are provided in Supplementary Table S12), are indicated by a single black asterisk $^{*}p < 0.05$, or three black asterisk $^{***}p < 0.0001$.

exposure ($p \le 9 \times 10^{-5}$, Tukey's honest significant difference criterion, *p*-values and test details in Supplementary Table S12). At the end of the experiment (45 min After), E'' for cells treated with isoflurane or flowing air was significantly lower than E'' for the no flow control cells ($p \le 0.02$, Tukey's honest significant difference criterion, *p*-values and test details in Supplementary Table S12). This observation suggests that prolonged gas flow increases neuronal E''. Together, these observations suggest that isoflurane increases neuronal E' and E'' both during and after exposure. However, at 45 min of recovery from isoflurane, alterations to neuronal E'' are due to gas flow, rather than the anaesthetic.

Based on the plots in Fig. 3a, b, it seems that E' and E'' are higher for neurons exposed to flowing gas compared to no flow control cells. However, as shown in Supplementary Table S12, this difference is not statistically significant. The lack of significance is due to large heterogeneity in E' and E'' between individual cells, both in these and literature[24] measurements. While the mean and standard error appear lower for no flow control cells, cell-cell heterogeneity renders this difference insignificant.

Neuronal E', E'' and $\tan\delta$ did not vary significantly across experimental time points for no flow control cells. As shown in Supplementary Table S13, E', E'' and $\tan\delta$ of flowing air control cells also did not vary through time, save for a slight increase in E'' between the 15 min During and 45 min After time points (Tukey's honest significant difference criterion, details in Supplementary Table S13). This observation supports the notion that gas flow increases neuronal E''. Isoflurane increased neuronal E' and E'' during and after exposure to the anaesthetic. As shown in Fig. 3a, b, the increase in E' was more pronounced, and peaked at 45 min during isoflurane exposure ($p \le 0.01$, Tukey's honest significant difference criterion, individual *p*-values and details in Supplementary Table S13). The increase in E'' was delayed compared to E', and peaked 30 min after isoflurane exposure ($p \le 0.05$, Tukey's honest significant difference criterion, individual *p*-values and details in Supplementary Table S13).

Neuronal $\tan\delta$ was also significantly ($p = 0.0002$, ANOVA, Supplementary Table S11) affected by experimental treatment (Fig. 3c and Supplementary Table S11). However, individual *post hoc* comparisons between time points were not statistically significant (test details in Supplementary Table S13). This observation is likely due to the fact that the range in neuronal $\tan\delta$ values, 0.4-1.7 for these experiments and the literature[24], was much smaller than that of E' and E'', which ranged several orders of magnitude. Since the range in $\tan\delta$ values is much smaller, differences in $\tan\delta$ between time points are more subtle than differences in E' or E''. Therefore, more cells would need to be measured for individual $\tan\delta$ comparisons to be significantly different. However, since $\tan\delta = E''/E'$, and since E' and E'' differ significantly between time points, it is reasonable to conclude that the ANOVA results in Supplementary Table S11 are accurate, and hence $\tan\delta$ varies through time, depending on experimental treatment. Isoflurane initially decreased $\tan\delta$ (30 min During) due to the increase in neuronal E' at this time point, and increased it at 45 min of isoflurane exposure due to the delayed increase in neuronal E''.

Correlation between neuron viscoelasticity and firing. In order to examine the relationship between neuron firing and viscoelasticity, linear regression was performed on the mean number of times a neuron fired vs. the mean neuronal E', E'' or $\tan\delta$ measured at a given frequency. Regression was performed on the data from cells treated with isoflurane and the flowing air control in During and After time points (details in Materials and Methods). Figure 4 shows that the mean number of firing events is linearly proportional to neuronal $\tan\delta$ measured at frequencies below 7.5 Hz. This correlation between neuronal firing and $\tan\delta$ is significant (regression p-values in Supplementary Table S14, all $p < 0.04$). As shown in Supplementary Figs. S9 and S10, and confirmed by the regression p-values in Supplementary Table S14, neither E' nor E'' correlate with mean number of firing events. Similarly, points excluded from the regression (Before and no flow measurements) do not have a linear relation with neuron mechanics, as shown in Supplementary Figs. S11–S13, due to the additional confounding variables of temperature and absence of gas flow (as previously discussed).

While the relationship between neuronal firing and $\tan\delta$ was significant, a large amount of variation in the data is not explained by the correlation. For regressions with significant p-values, R^2 and root mean square error (RMSE) values ranged between 0.44–0.70 and 0.16 and 0.22, respectively (individual values can be found in Supplementary Table S14). The unexplained variation is likely due to cell–cell heterogeneity, since E' and E'' respectively ranged within 0.1–4 kPa and 0.05–3 kPa, $\tan\delta$ ranged within 0.1–1.6, and the number times a cell fired at any given time point ranged between 0 and 20 (Supplementary Fig. S5). Due to this cell-cell heterogeneity, it is expected that the correlation would not explain all variation in the data, even while being statistically significant.

It is worth emphasising that, while $\tan\delta$ is the focus of this work, linear regression p-values for E' alone were also small, with $p \approx 0.1$ for some frequencies (exact values can be found in Supplementary Table S14). These p-values were smaller than those of E'' (Supplementary Table S14), as E' changed more than E'' in response to isoflurane (Fig. 3a, b). While it is tempting to interpret the small p-values for E' as implying a linear relationship between cell firing and E', the relationship is not linear, as shown in Supplementary Figs. S9 and S10. Since E' changed more in response to isoflurane than E'', one could potentially consider E' as the primary correlation variable. However, doing so ignores the fact that changes in E'' did still occur (Fig. 3(b)). Therefore, focusing on $\tan\delta = E''/E'$ is useful because $\tan\delta$ exhibits the simplest, linear, correlation and ensures that dissipative properties of cells are accounted for in addition to storage properties.

Summary and Implications. Isoflurane affects both neuron firing and viscoelasticity. Neuronal firing was altered, rather than dampened, in the presence of isoflurane (Fig. 2 and Supplementary Figs. S5–S7, Supplementary Tables S3–S10). These findings agree with EEG measurements[12,13]. Simultaneously, isoflurane increased neuronal E' and E''. Changes in E'' occurred to a lesser extent and with a 15–30 min delay compared to E' (Fig. 3 and Supplementary Table S13). This delay is characteristic of cell mechanics, and is hypothesised to arise from bond binding/unbinding dynamics in the cytoskeleton as a cell transitions from one energetic state to another[25]. The fact that isoflurane altered cell mechanics in such a manner supports the hypothesis that general anaesthetics affect intermolecular interactions within a cell[10,11] and suggests that general anaesthetics exert their effect on cell activities by altering cell thermodynamics at a systemic level. Additionally, the observed linear correlation between changes in neuron firing and $\tan\delta$ (Fig. 4 and Supplementary Table S14) suggests that neuron firing and mechanics are coupled. These observations have several implications for anaesthesia, neuroscience in general, and clinical neuroscience.

Implications for anaesthesia. Cells contain multiple components and processes. Mechanical properties measured at frequency f are largely determined by components and processes that operate on timescales $\tau \approx 1/f$[17,26,27]. Neuron firing correlated with neuronal $\tan\delta$ for $f = 0.5$–5 Hz (Supplementary Table S14), hence for processes with $\tau \approx 0.2$–2 s. Cellular processes that operate on such timescales are protein and other molecular interactions such as those that occur in molecular complexes, cytoskeleton assembly and disassembly, protein folding and cell signalling[28–33]. These observations again support the hypothesis that isoflurane alters intermolecular interactions of multiple subcellular components[1,3,10,11]. Additionally, gene translation occurs with $\tau \geq 10$ s[28]. The frequencies in this study have a similar order of magnitude (2 s), and thus raise the possibility that isoflurane could affect transcription. In fact, this hypothesis agrees with literature demonstrating that isoflurane affects transcription initiation and gene expression[34–39]. Therefore, our results demonstrate that multiple cellular processes are affected by isoflurane.

Furthermore, both lipid-mediated and protein-mediated mechanisms have historically been proposed to explain the effects of general anaesthetics, though without reaching a consensus[3]. Similarly, changes to the cell cytoskeleton have also proposed to explain anaesthetic effects[11,17,25]. The results in this study reconcile these different theories by demonstrating that anaesthetics alter the state of the cell as a whole, instead of affecting only one specific component.

While this study used isoflurane, an inhalational anaesthetic, intravenous anaesthetics also affect multiple cellular components[40–44]. Therefore, cellular responses to intravenous anaesthetics likely also involve changes in cell mechanics. However, inhalational and intravenous anaesthetics can cause different, and sometimes opposite, changes in cell signalling pathways[44,45]. Future avenues for this work could thus characterise how cell firing and mechanics change in response to liquid anaesthetic agents, and compare these changes to those caused by inhalational anaesthetics.

Implications for neuroscience in general. A growing body of literature suggests that cells, and in particular the cell membrane, may exist on the boundary of a phase transition between a solid- and fluid-like state[15,16,46]. Building on this observation, action potentials have been suggested to be linked to transient phase changes that propagate along the cell[15,16]. Such shifts in neuronal phase and action potential propagation may in fact be experimentally detectable by observing changes in $\tan\delta$, related to mechanical phase changes via the time-temperature superposition principle[17]. However, in order to confirm or deny this hypothesis, $\tan\delta$ must either be measured over a wider range of frequencies using techniques such as nano-DMA atomic force microscopy[47], or additional modelling must be involved[17].

Regardless, the observed correlation between neuron firing and $\tan\delta$ demonstrates that considering action potentials from an energetic perspective is useful. In the traditional view of neuron electrophysiology, action potentials propagate via ionic flows adjacent to and across the membrane via conformational changes of ion channels[14,48]. From an energetic perspective, some energy from the stimulus is thus stored by the membrane, allowing ion channels to open/close and the membrane to alter voltage, while the rest is dissipated (e.g., as heat arising from kinetic energy in a viscous medium and/or biochemical bond release) and potentially reabsorbed during propagation[15], dictating how the action potential travels down the membrane, and how the membrane

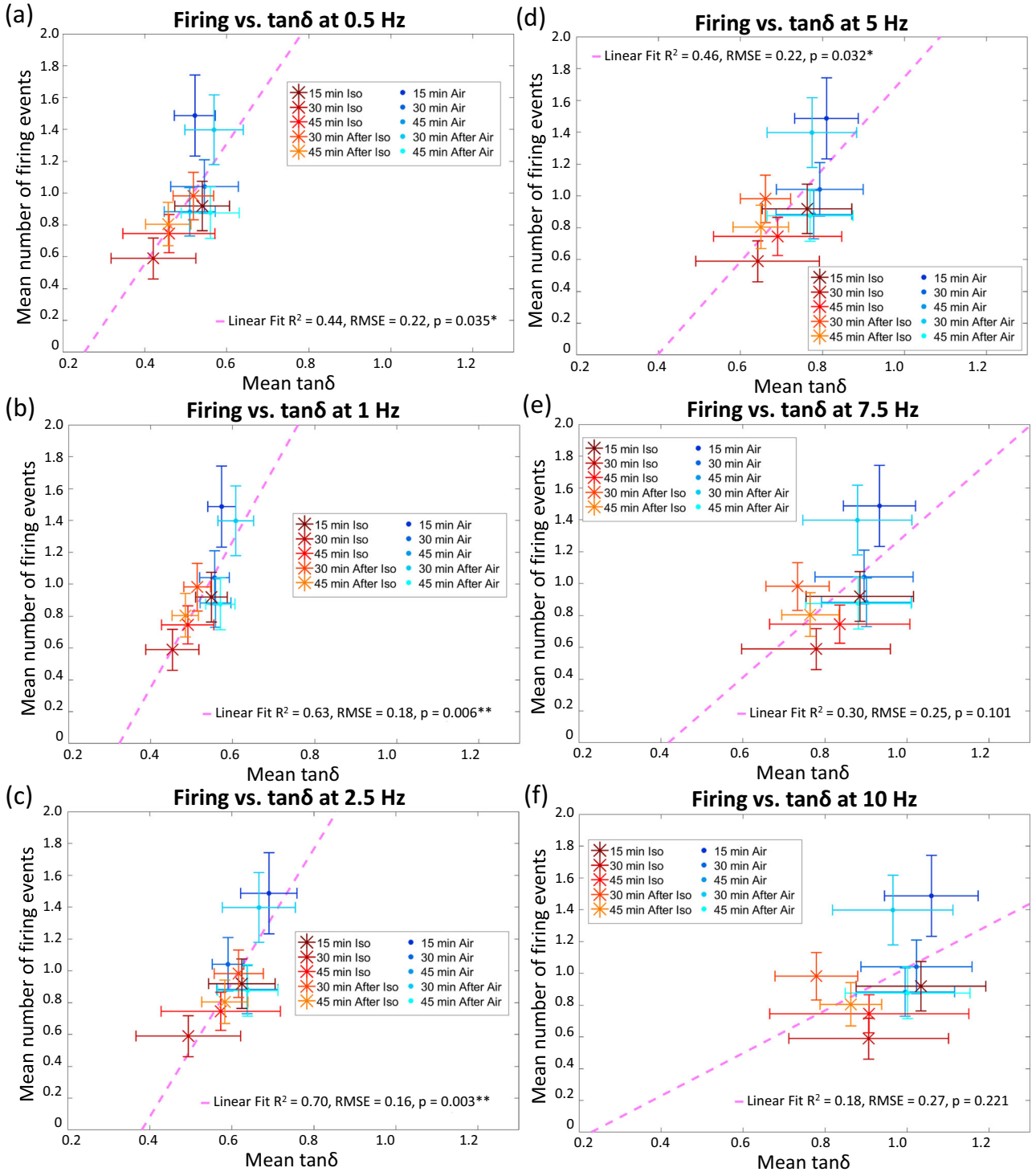

Fig. 4 Correlation between neuronal firing and loss tangent. Neurons were treated with isoflurane (iso, red/yellow asterisk), or flowing air (air, blue/cyan points) as a control. Linear regression (pink dashed lines) was performed on the mean number of times neurons fired vs. mean neuronal loss tangent (tan δ) measured at: 0.5, 1, 2.5, 5, 7.5 or 10 Hz, shown in **a**–**f**, respectively. Linear regression (metrics shown in each panel and in Supplementary Table S14) was performed on measurements collected at five experimental time points: 15, 30 and 45 min during gas exposure, and 30 and 45 min after gas exposure (indicated by point shading). Measurements before gas exposure were excluded because the sample was at a higher temperature during Before measurements than during subsequent measurements. Similarly, control measurements of no gas flow were excluded from the regression in order to avoid convoluting the effects of isoflurane with those of the flow itself. Significant correlations are indicated by: $^{*}p < 0.05$ and $^{**}p < 0.005$.

attenuates the impulse[17]. Both energy storage and dissipation are thus required for action potential propagation.

The traditional electrical-only characterisation of action potentials is increasingly challenged due to observations of mechanical, chemical, heat and pH changes accompanying the electrical wave[3,15,16,49]. Therefore, the consideration of action potentials from an energetic perspective is particularly fitting, since all physical properties define how a cell stores, dissipates or transfers energy.

For instance, E' quantifies the mechanical potential energy per unit volume of the sample that acts to restore the original sample configuration when the stimulus is removed, while E'' quantifies the energy per unit volume dissipated by the sample in response to the stimulus[17,27,50,51]. The ratio between both quantities, $\tan\delta$, is a measure of mechanical damping (higher $\tan\delta$ means more damping) by the material[17]. In traditional mechanics, dissipation is often associated to an actual transfer of the energy into heat. In view of the multiphysics properties of action potentials, and in agreement with Onsager's variational principle[27], our framework does not preclude a transfer (reversible or not) of mechanical energy into another form not necessarily linked to heat, such as biochemical. The observed correlation between $\tan\delta$ and the number of times a neuron fires shows that, for a neuron to fire, the cell must store enough energy that the cytoskeleton and membrane deform and depolarise in response to a stimulus, but also dissipate enough that the signal is able to propagate. The consideration of energy storage and dissipation relative to each other is paramount, rather than either quantity alone. Thus, measurements of neuronal $\tan\delta$ likely provide insights into how neurons fire in general.

The changes we observed in neuron mechanics are characteristic of a shift in the thermodynamic state of the cell and its cytoskeleton[25], thereby suggesting that isoflurane shifts the thermodynamic state of neurons[17]. This is in agreement with recent work demonstrating how membrane phase changes correlate with electrophysiological properties[46]. As such, neuronal $\tan\delta$ can not only provide insight into how action potentials propagate, but also into phase changes and firing activity within neurons.

Clinical implications. Our results may help elucidate a number of still unexplained phenomena in anaesthesia. For example, general anaesthetics have deleterious effects on neurodevelopment[52], and increase the risk of tumour recurrence[53,54]. Since cell mechanics play a role in dictating development[55] and cancer progression[56], it is plausible that general anaesthetics affect these processes via the changes general anaesthetics induce to cell mechanics. Additionally, it is possible that cellular contents and short-term gene expression[34–39] are altered as a direct result of the isoflurane, or as a secondary effect of the changes in neuron mechanics. Again, this may help explain why general anaesthetics affect development and cancer progression. Regardless, our results demonstrate a direct link between cellular mechanics and general anaesthetics, potentially motivating the need for new considerations when selecting and administering anaesthetics.

Taken together, our results also indicate that $\tan\delta$ measurements could provide insight into how a neuron is likely to function in the presence of anaesthetics, and thereby support improvements in anaesthetic design, dosage and effectiveness. Additionally, these results raise the possibility that other treatments, and possibly disease states, exert their effects by altering neuronal $\tan\delta$. If so, it may be possible to design novel therapies that indirectly treat various conditions by modulating neuronal $\tan\delta$.

Conclusion

Here, we used a custom experimental approach combining nanoindentation with fluorescence imaging to quantify changes in neuronal viscoelasticity and firing in response to clinically relevant concentrations of general anaesthetics. Doing so, we demonstrated that isoflurane simultaneously alters both cell mechanics and firing. In particular, alterations in firing counts correlate linearly with alterations in $\tan\delta$. These results suggest that general anaesthetics alter intermolecular interactions within subcellular components, thus altering the state of the cell as a whole. Additionally, these results show that, in order to understand the mechanism by which drugs such as general anaesthetics operate, joint consideration of cell electrophysiology and mechanics as concurrent and collaborative actors is required. Further understanding of the correlation between neuron firing and $\tan\delta$ may allow for the design of new treatments for neurological diseases by modulating neuronal $\tan\delta$.

Materials and methods

Cell culture. F11 cells (ECCAC 08062601, UK)[57] between passage 21 and 32 were cultured in a humidified incubator at 37 °C in 5% CO_2. To create sensory neurons, F11 cells, a hybrid between mouse N18TG-2 neuroblastoma and embryonic rat dorsal root ganglion neurons, were seeded in 50 mm glass bottom petri dishes (Wilco Wells HBST-5040) at a density of 1×10^5 cells per dish, in 2 mL of differentiation medium and allowed to differentiate for four days. Every other day, 1 mL of the differentiation medium was replaced with 1 mL of fresh differentiation medium. Differentiation medium consisted of Dulbecco's modified Eagle medium (DMEM, ThermoFisher 11995-065), 1% foetal bovine serum (FBS, ThermoFisher 10500064), and 1% penicillin/streptomycin (P/S, ThermoFisher 15140122) supplemented with 2 µM Retinoic Acid (RA, Sigma-Aldrich R2625), 10 µM 3-isobutyl-1-mythylxanthine (IBMX, Sigma-Aldrich I5879), 0.5% Insulin Transferrin Selenium (ITS, ThermoFisher 51300044), 50 ng/mL nerve growth factor (NGF, Prepotech 450-01) and 0.5 mM 8-Bromoadenosine $3' - 5'$ cyclic monophosphate (8-Bromo-cAMP, Sigma-Aldrich B5386)[57,58]. Mature cells on the fifth and sixth day of differentiation exhibit spontaneous firing activity[19,57,58], and are established models of sensory neurons[57–61]. All experiments were performed on differentiation day 5 or 6.

Custom experimental setup and data recording. A custom experimental apparatus, shown in Fig. 1a, b, was used to measure the effects of isoflurane on differentiated neurons. The apparatus combined a Chiaro nanoindenter (Optics11) with an inverted microscope (Nikon Eclipse Ti) in order to measure neuron viscoelasticity and calcium imaging activity, respectively. This apparatus has previously been employed to measure electromechanical coupling in neurons[18–20]. The setup was enclosed in a gas tight box in order to safely contain the isoflurane. Temperature control was not employed in this setup because the controller added too much vibrational noise to nanoindenter measurements.

Isoflurane was delivered to cells via a custom flow system similar to what is used in the clinic[2]. The flow system consisted of a syringe pump, vaporiser, gas tight box containing the sample, and waste scavenging system, all connected via sealed tubing as shown in Fig. 1a. A 50 mL syringe containing liquid isoflurane was loaded into the syringe pump and connected to the vaporiser via tubing. Upon activating the pump, isoflurane was delivered to the vaporiser at a constant rate of 3.5 mL/h. In the vaporiser, all of the liquid isoflurane vaporised and joined a stream of compressed air, which entered the vaporiser via a connection between the vaporiser and a compressed air cylinder. The gas flow rate out of the vaporiser was set to 1 L/min, ensuring that a gaseous mixture of 1% isoflurane in air (by volume), a widely-used clinical concentration[12,62], was delivered to the sample. From the vaporiser, the gaseous mixture of ~1% isoflurane flowed into the gas tight box containing the sample, then out of the box into an activated charcoal scavenger (Harvard Apparatus 34-0415) which captured the isoflurane and rendered the anaesthetic inert. Turning the syringe pump on or off respectively started or stopped exposing the sample to isoflurane.

Note that calculating the exact isoflurane concentration in cells is not straightforward, but can be estimated by multiplying the chamber concentration (1%) by isoflurane's partition coefficient for a particular medium. For example, isoflurane's blood:gas partition coefficient is 1.45:1[63]. Since culture medium contains salt concentrations similar to average levels in the blood, the concentration of isoflurane in the culture medium is roughly 1.45%. To calculate the concentration of isoflurane inside cells, isoflurane's partition coefficient in the cell and/or all subcellular components (such as the membrane:gas, cytoskeleton:gas, nucleus:gas, etc. partition coefficients) must be known. Cellular partition coefficients are difficult to measure, thereby preventing exact calculation of the isoflurane concentration inside cells. However, using isoflurane's blood:gas partition coefficient, the isoflurane concentration in cells can be estimated as greater than or equal to 1.45%.

Two control experiments were carried out. First, in order to determine the effects of isoflurane, a flowing air control was performed by filling the syringe with room air instead of isoflurane and establishing gas flow via the syringe pump in the same manner as that for isoflurane. The second no flow control was performed in order to determine whether gas flow through the setup affected the measurements. In this control, a syringe full of room air was placed on the syringe pump and all the tubing remained in place. However, the gas cylinder was never opened and the syringe pump was never activated during the no flow control experiments.

As shown in Fig. 1c, measurements of neuron viscoelasticity, via dynamic mechanical analysis (DMA), or firing, via calcium imaging, were performed at six different time points throughout the experiment. Only one technique was used on any given sample, in order to minimise the likelihood that the DMA probe interfered with neuron firing measurements, or that the imaging dye interfered with cell mechanics measurements. As shown in Supplementary Figure S4 and Supplementary Table S1, the calcium imaging dye does not alter cell viscoelasticity. However, mechanical stimuli at the frequencies used for DMA measurements alter

cell firing[19]. Therefore, separate measurements ensure that changes in cell firing are due to the isoflurane, not the mechanical deformations during DMA measurements. For cells exposed to the isoflurane or the flowing air control, DMA or calcium imaging was performed on cells before the syringe pump was activated. The syringe pump was then activated to begin exposing the cells to the contents of the syringe. Measurements during exposure were performed at time points of 15, 30 and 45 min after the pump was activated. Next, the pump was deactivated, and additional measurements were collected 30 min and 45 min after the pump had stopped. For the no flow control, the same six time points were maintained, but the gas cylinder was never opened and the syringe pump was never activated.

For each experiment, the cells were removed from the incubator (37 °C) and placed inside the gas tight box of the experimental apparatus. The box was sealed, and the Before measurement was collected. Since ambient temperature was ~13–18 °C and temperature control could not be applied (the controller caused vibrational noise interfering with the DMA measurements), cells were slightly warmer during the Before measurement than they were at subsequent time points. While a longer Before phase could have been considered to ensure that the cells were fully cooled down to ambient temperature, the total length of each experiment (96 min) had to be accounted for, and the current approach was adopted to minimise neuronal death during the duration of the experiments.

Calcium imaging. Calcium imaging was used to measure the effects of isoflurane on neuron firing. When a neuron fires, a surge of calcium is released into the cytoplasm[64–67]. In calcium imaging, a dye which emits light only in the presence of calcium is allowed to diffuse into cell cytoplasms[68]. Spikes in fluorescence thus indicate a surge of calcium in the cytoplasm, which typically emerges from neuronal firing[68]. A single spike in fluorescence intensity is considered to be a single firing event, called a functional event, which arises from one or more action potentials[69].

Differentiated F11 cells were incubated at 37 °C in PBS containing Oregon Green 488 BAPTA (ThermoFisher O6807) for 1 h to allow the dye to diffuse into cell cytoplasms[68]. The PBS was then replaced with 2 mL FluoroBrite DMEM imaging media (ThermoFisher, A1896701) and the cells were incubated at 37 °C for another 35 min to allow cell esterases to functionalise the dye[68]. Cells were then moved to an inverted microscope (Nikon Eclipse Ti). At each of the six experimental time points (Fig. 1b), a 2–3 min movie of Oregon Green 488 BAPTA fluorescence in the microscope's field of view (×10 objective, containing a few hundred cells) was recorded with a frame rate and exposure time of 400 ms. Representative images of neurons and the corresponding Oregon Green 488 BAPTA fluorescence are shown in Supplementary Fig. S3. All six movies were then analysed and processed in a custom MATLAB R2019a script, detailed in Supplementary Note 2. This script segmented out individual cells in the field of view and assigned each cell a unique ID (details in Supplementary Note 2.1), tracked cells between the six different movies/experimental time points (details in Supplementary Note 2.2), then detected and counted fluorescence spikes in each individual cell (details in Supplementary Note 2.3). A schematic of this procedure is shown in Supplementary Figure S1a. Ten dishes treated with isoflurane, eight dishes treated with the flowing air control, and six dishes treated with the no flow control were measured. Not all F11 cells assume a neuronal phenotype upon differentiation. To avoid measuring cells that failed to become neurons, cells that never fired were discarded from analysis. A total of 184 cells exposed to isoflurane, 169 cells exposed to flowing air and 151 cells exposed to the no flow control were used in the data analysis.

Dynamic mechanical analysis. Nanoindenters are experimental tools that can be used to measure cellular mechanics in physiological (hydrated and unprocessed) conditions[70]. Nanoindenters apply deformations to a sample via a tip with a microscale diameter attached to a cantilever, and measure the sample's response via interferometry[70–73]. While nanoindenters can perform many different types of mechanical measurements, dynamic mechanical analysis (DMA) is performed in this work to measure neuronal storage modulus E', loss modulus E'' and loss tangent $\tan\delta$, which depend on the frequency of the applied stimulus[27,47,50,70]. E' (Pa) measures the contribution of the sample's response that is in-phase with the applied stimulus, and quantifies the potential energy per unit volume of the sample that acts to restore the original sample dimensions when the stimulus is removed[17,27,50,51]. E'' (Pa) measures the contribution of the sample's response that is out-of-phase with the applied stimulus, and quantifies the energy per unit volume dissipated (often as heat) by the sample during mechanical stimulus[17,27,50,51]. The ratio between both quantities, $\tan\delta$, is a measure of mechanical damping (higher $\tan\delta$ means more damping) by the material[17]. While the values of E' and E'' depend on the contact geometry of the tip/sample interaction[47,50,70], the geometrical terms cancel out in $\tan\delta$, thereby rendering $\tan\delta$ independent of the geometry of the tip/sample interaction. Therefore, $\tan\delta$ is less prone than E' and E'' to experimental error arising from uncertainty in the contact geometry[47,50,70].

The DMA procedure in this work was as follows. Before DMA measurements, neuron differentiation medium was replaced with 2 mL of FluoroBrite DMEM imaging media (ThermoFisher, A1896701) to keep conditions consistent for both calcium imaging and DMA measurements. E', E'' and $\tan\delta$ values of a single neuron were measured at different experimental time points via microscale DMA applied by a Chiaro nanoindenter (Optics11) operated in displacement control mode. Nanoindenter probes (Optics11, P-Chiaro-MN2-TN1-ST) consisted of a tip with a 10 ± 1 μm radius (mean ± standard deviation) attached to a cantilever with a stiffness of 0.025 ± 0.002 N/m (mean ± standard deviation). In general, to perform DMA, cells were indented, separate oscillations at six different frequencies were applied around the initial indentation depth, then the cantilever was withdrawn from the cell until the next measurement, as shown in Supplementary Fig. S1b. Specifically, cells were indented at a velocity of 0.20 μm/s until the cantilever experienced a force of 0.01 μN ± 0.001 μN (mean ± standard error). This resulted in an initial indentation depth of a few microns. The cell was then allowed to relax for 30 s before any DMA measurements were collected[19]. DMA was performed by applying a sinusoidal compression with a displacement amplitude of 400 nm and a frequency of: 0.5, 1, 2.5, 5, 7.5 or 10 Hz. The cell was allowed to relax for at least 10 s between each DMA frequency. Since the cell membrane is ~5 nm thick[74], the applied DMA oscillations, as well as the initial indentation, deformed and measured intracellular components in addition to the lipid bilayer membrane. Therefore, the measured E' and E'' represent whole-cell properties arising from the combined membrane, cytoskeleton and possibly nucleus of the neuron. Once measurements at each frequency were performed, the tip was retracted from the cell at a retraction velocity of 0.20 μm/s. The tip was left out of contact with the cell until DMA measurements were repeated at the next experimental time point. The same cell was measured throughout the experiment. E' and E'' were calculated for each measurement frequency in the Optics11 DataViewer 2.5 software by fitting the experimental force and indentation time signals and applying the following equations[70,75].

$$\frac{E'}{1-\nu^2} = \frac{1}{2}\frac{F_0}{h_0}\cos(\delta)\frac{1}{\sqrt{Rh}} \quad (1)$$

$$\frac{E''}{1-\nu^2} = \frac{1}{2}\frac{F_0}{h_0}\sin(\delta)\frac{1}{\sqrt{Rh}} \quad (2)$$

$$\tan\delta = \frac{E''}{E'} = \frac{\sin(\delta)}{\cos(\delta)} \quad (3)$$

Here, h is the indentation depth, h_0 is the amplitude of the applied deformation, F_0 is the amplitude of the force experienced by the sample, δ is the phase lag between the load and the displacement and ν is the Poisson's ratio of the sample[70,76]. Example recordings of h, h_0, F and F_0 from DMA of a single neuron are shown in Supplementary Fig. S2. Details on how h and F_0 are calculated from interferometer readings can be found in Supplementary Note 1, which describes the nanoindenter's working principle[70–73,75].

Three controls were used to ensure that only healthy neurons were measured. First, the measurement at 1 Hz was performed at the start and end of the frequency sweep to ensure that the cell was not damaged during the measurements. If the 1 Hz E', E'' and $\tan\delta$ were not consistent within a single measurement, it was assumed that the cell had been irreversibly altered (likely damaged) during the DMA sweep, and data from the cell were discarded from analysis. Second, only cells with large, spherical somas and neurite elongations were measured in order to ensure that the measured cell was healthy and differentiated. Third, only isolated cells without neighbours were measured in order to minimise the effect of neighbouring cells on E', E'' and $\tan\delta$. At least three cells were measured for each treatment, in order to account for cell-cell variability. Five cells treated with isoflurane, five cells treated with the flowing air control, and three cells treated with the no flow control were measured.

Statistical analysis. Results are shown as mean ± standard error. Statistical analysis was performed in a custom MATLAB R2019a script. A Shapiro-Wilk test was used to test the normality of the distributions. For normally distributed data, analysis of variance (ANOVA) followed by a *post hoc* Tukey's honest significant difference criterion test were used to calculate significant differences between the six experimental time points and three treatments. For data which did not follow a normal distribution, a Kruskal–Wallis test followed by Wilcoxon Rank Sum tests were used to calculate comparison p-values. Comparisons were considered significantly different if the p-value was <0.05.

Linear regression was performed in order to quantify the correlation between neuron firing and neuronal E', E'' or $\tan\delta$. Data points for the linear regression consisted of x = the mean E', E'' or $\tan\delta$ at a particular frequency (0.5, 1, 2.5, 5, 7.5 or 10 Hz) and y = the mean number of firing events at each experimental time point. In order to reduce the effect of experimental variability due to gas flow, and isolate the effect of isoflurane alone, no flow control measurements were excluded from the regression, to avoid convoluting the effects of gas flow with those of isoflurane. Additionally, since Before measurements were collected at a different temperature from subsequent time points, the Before values were not included in the fits in order to avoid convoluting the effects of temperature with those of isoflurane. To conclude, only the air flow and isoflurane flow values in the During and After periods were included in the linear regression.

Reporting summary. Further information on research design is available in the Nature Portfolio Reporting Summary linked to this article.

Data availability

Experimental data, and data analysis codes, are available upon request.

Received: 7 September 2022; Accepted: 24 May 2023;
Published online: 12 July 2023

References

1. Baluška, F., Yokawa, K., Mancuso, S. & Baverstock, K. Understanding of anesthesia - Why consciousness is essential for life and not based on genes. *Commun. Integr. Biol.* **9**, e1238118 (2016).
2. Vats, A. & Marbaniang, M. J. *Surgery (United Kingdom)* (Elsevier Ltd., 2019).
3. Jerusalem, A. et al. Electrophysiological-mechanical coupling in the neuronal membrane and its role in ultrasound neuromodulation and general anaesthesia. *Acta Biomater.* **97**, 116–140 (2019).
4. Culley, D. et al. Isoflurane affects the cytoskeleton but not survival, proliferation, or synaptogenic properties of rat astrocytes in vitro. *Br. J. Anaesth.* **110**, i19–i28 (2013).
5. Patel, J., Chowdhury, E. A., Noorani, B., Bickel, U. & Huang, J. Isoflurane increases cell membrane fluidity significantly at clinical concentrations. *Biochim. Biophys. Acta - Biomembr.* **1862**, 183140 (2020).
6. Yoo, K. Y. et al. The effects of volatile anesthetics on spontaneous contractility of isolated human pregnant uterine muscle: a comparison among sevoflurane, desflurane, isoflurane, and halothane. *Anesth. Analg.* **103**, 443–447 (2006).
7. Pavel, M. A., Petersen, E. N., Wang, H., Lerner, R. A. & Hansen, S. B. Studies on the mechanism of general anesthesia. *Proc. Natl Acad. Sci. USA* **117**, 13757–13766 (2020).
8. Ono, J. et al. Effect of the volatile anesthetic agent isoflurane on lateral diffusion of cell membrane proteins. *FEBS Open Bio* **8**, 1127–1134 (2018).
9. Deng, Q., Liu, L. & Sharma, P. Flexoelectricity in soft materials and biological membranes. *J. Mech. Phys. Solids* **62**, 209–227 (2014).
10. Turin, L., Skoulakis, E. M. C. & Horsfield, A. P. Electron spin changes during general anesthesia in Drosophila. *Proc. Natl Ac. Sci. USA* **111**, E3524–E3533 (2014).
11. Hameroff, S. R. The entwined mysteries of anesthesia and consciousness. *Anesthesiology* **105**, 400–412 (2006).
12. Hagihira, S. Changes in the electroencephalogram during anaesthesia and their physiological basis. *Br. J. Anaesth.* **115**, i27–i31 (2015).
13. Zhang, Z. et al. Isoflurane-induced burst suppression increases intrinsic functional connectivity of the monkey brain. *Front. Neurosci.* **13**, 296 (2019).
14. Hodgkin, A. L. & Huxley, A. F. A quantitative description of membrane current and its application to conduction and excitation in nerve. *J. Physiol.* **117**, 500–544 (1952).
15. Heimburg, T. The thermodynamic soliton theory of the nervous impulse and possible medical implications. *Prog. Biophys. Mol. Biol.* https://linkinghub.elsevier.com/retrieve/pii/S0079610722000529 (2022).
16. Drukarch, B., Wilhelmus, M. M. M. & Shrivastava, S. The thermodynamic theory of action potential propagation: a sound basis for unification of the physics of nerve impulses. *Rev. Neurosci.* **33**, 285–302 (2022).
17. Nielsen, L. E. *Mechanical Properties of Polymers and Composites*, (M. Dekker, New York, 1974).
18. Kayal, C., Tamayo-Elizalde, M., Adam, C., Ye, H. & Jerusalem, A. Voltage-driven alterations to neuron viscoelasticity. *Bioelectricity* https://doi.org/10.1089/bioe.2021.0028 (2022).
19. Tamayo-Elizalde, M., Chen, H., Malboubi, M., Ye, H. & Jerusalem, A. Action potential alterations induced by single F11 neuronal cell loading. *Progress in Biophysics and Molecular Biology* (2020).
20. Tamayo-Elizalde, M., Kayal, C., Ye, H. & Jérusalem, A. Single cell electrophysiological alterations under dynamic loading at ultrasonic frequencies. *Brain Multiphys.* **2**, 100031 (2021).
21. Roca-Cusachs, P. et al. Rheology of passive and adhesion-activated neutrophils probed by atomic force microscopy. *Biophys. J.* **91**, 3508–3518 (2006).
22. Yu, Y., Hill, A. P. & McCormick, D. A. Warm body temperature facilitates energy efficient cortical action potentials. *PLoS Comput. Biol.* **8**, 1–16 (2012).
23. Buzatu, S. The temperature-induced changes in membrane potential. *Riv. Biol.* **102**, 199–217 (2009).
24. Lu, Y.-B. et al. Viscoelastic properties of individual glial cells and neurons in the CNS. *Proc. Natl Acad. Sci. USA* **103**, 17759–17764 (2006).
25. Trepat, X., Lenormand, G. & Fredberg, J. J. Universality in cell mechanics. *Soft Matter* **4**, 1750 (2008).
26. Seifert, J., Kirchhelle, C., Moore, I. & Contera, S. Mapping cellular nanoscale viscoelasticity and relaxation times relevant to growth of living Arabidopsis thaliana plants using multifrequency AFM. *Acta Biomater.* **121**, 371–382 (2021).
27. Doi, M. *Soft Matter Physics*. 1st edn (Oxford University Press, 2013).
28. Shamir, M., Bar-On, Y., Phillips, R. & Milo, R. SnapShot: timescales in cell biology. *Cell* **164**, 1302–1302.e1 (2016).
29. Secrier, M. & Schneider, R. Visualizing time-related data in biology, a review. *Brief. Bioinform.* **15**, 771–782 (2014).
30. Lee, R. M. & Losert, W. Dynamics phenotyping across length and time scales in collective cell migration. *Semin. Cell Dev. Biol.* **93**, 69–76 (2019).
31. Jünger, F. & Rohrbach, A. Strong cytoskeleton activity on millisecond timescales upon particle binding revealed by ROCS microscopy. *Cytoskeleton* **75**, 410–424 (2018).
32. Doong, J., Parkin, J. & Murray, R. M. Length and time scales of cell-cell signaling circuits in agar. *Synth. Biol.* http://biorxiv.org/lookup/doi/10.1101/220244 (2017).
33. Cadart, C., Venkova, L., Recho, P., Lagomarsino, M. C. & Piel, M. The physics of cell-size regulation across timescales. *Nat. Phys.* **15**, 993–1004 (2019).
34. Upton, D. H., Popovic, K., Fulton, R. & Kassiou, M. Anaesthetic-dependent changes in gene expression following acute and chronic exposure in the rodent brain. *Sci. Rep.* **10**, 9366 (2020).
35. Lowes, D. A., Galley, H. F., Moura, A. P. & Webster, N. R. Brief isoflurane anaesthesia affects differential gene expression, gene ontology and gene networks in rat brain. *Behav. Brain Res.* **317**, 453–460 (2017).
36. Bunting, K. M., Nalloor, R. I. & Vazdarjanova, A. Influence of isoflurane on immediate-early gene expression. *Front. Behav. Neurosci.* http://journal.frontiersin.org/Article/10.3389/fnbeh.2015.00363/abstract (2016).
37. Palmer, L. K., Shoemaker, J. L., Baptiste, B. A., Wolfe, D. & Keil, R. L. Inhibition of translation initiation by volatile anesthetics involves nutrient-sensitive gcn-independent and -dependent processes in yeast. *Mol. Biol. Cell* **16**, 3727–3739 (2005).
38. Rampil, I. J., Moller, D. H. & Bell, A. H. Isoflurane modulates genomic expression in rat amygdala. *Anesth. Analg.* **102**, 1431–1438 (2006).
39. Benzonana, L. L. et al. Isoflurane, a commonly used volatile anesthetic, enhances renal cancer growth and malignant potential via the hypoxia-inducible factor cellular signaling pathway in vitro. *Anesthesiology* **119**, 593–605 (2013).
40. Bensel, B. M., Guzik-Lendrum, S., Masucci, E. M. & Gilbert, S. P. Common general anesthetic propofol impairs kinesin processivity. *Proc. Natl Acad. Sci. USA* **114**, E4281–E4287 (2017).
41. D'Agostino, G. et al. Lidocaine inhibits cytoskeletal remodelling and human breast cancer cell migration. *Br. J. Anaesth.* **121**, 962–968 (2018).
42. Ma, J. et al. High-dose propofol anesthesia reduces the occurrence of postoperative cognitive dysfunction via maintaining cytoskeleton. *Neuroscience* **421**, 136–143 (2019).
43. Chang, H.-C., Chen, T.-L. & Chen, R.-M. Cytoskeleton interruption in human hepatoma hepg2 cells induced by ketamine occurs possibly through suppression of calcium mobilization and mitochondrial function. *Drug Metab. Dispos.* **37**, 24–31 (2009).
44. Iqbal, F. et al. Anesthetics: from modes of action to unconsciousness and neurotoxicity. *J. Neurophysiol.* **122**, 760–787 (2019). PMID: 31242059.
45. Huang, H. et al. Prostate cancer cell malignancy via modulation of hif-1α pathway with isoflurane and propofol alone and in combination. *Br. J. Cancer* **111**, 1338–1349 (2014).
46. Fedosejevs, C. S. & Schneider, M. F. Sharp, localized phase transitions in single neuronal cells. *Proc. Natl Acad. Sci. USA* **119**, e2117521119 (2022).
47. Piacenti, A. *Atomic Force Microscope-Based Methods for the Nano-Mechanical Characterisation of Hydrogels and other Viscoelastic Polymeric Materials for Biomedical Applications*. Ph.D. thesis (Oxford University, 2021).
48. Kress, G. & Mennerick, S. Action potential initiation and propagation: Upstream influences on neurotransmission. *Neuroscience* **158**, 211–222 (2009).
49. Hodgkin, A. L. *The Conduction Of The Nervous Impulse. No. 7 in Sherrington Lectures* (Liverpool University Press, 1964).
50. Popov, V. L., Heß, M. & Willert, E. *Handbook of Contact Mechanics: Exact Solutions of Axisymmetric Contact Problems*. (Springer Berlin Heidelberg, 2019).
51. Seifert, J. *In Vivo Dynamic AFM Mapping Of Viscoelastic Properties Of The Primary Plant Cell Wall*. DPhil (University of Oxford, 2018).
52. Liu, X., Ji, J. & Zhao, G.-Q. General anesthesia affecting on developing brain: evidence from animal to clinical research. *J. Anesth.* **34**, 765–772 (2020).
53. Wall, T., Sherwin, A., Ma, D. & Buggy, D. Influence of perioperative anaesthetic and analgesic interventions on oncological outcomes: a narrative review. *Br. J. Anaesth.* **123**, 135–150 (2019).
54. Montejano, J. & Jevtovic-Todorovic, V. Anesthesia and cancer, friend or foe? A narrative review. *Front. Oncol.* **11**, 803266 (2021).
55. Barriga, E. H., Franze, K., Charras, G. & Mayor, R. Tissue stiffening coordinates morphogenesis by triggering collective cell migration in vivo. *Nature* **554**, 523–527 (2018).
56. Suresh, S. Biomechanics and biophysics of cancer cells. *Acta Biomater.* **3**, 413–438 (2007).
57. Francel, P. C. et al. Neurochemical characteristics of a novel dorsal root ganglion X neuroblastoma hybrid cell line, F11. *J. Neurochem.* **48**, 1624–1631 (1987).
58. Boland, L. M. & Dingledine, R. Expression of sensory neuron antigens by a dorsal root ganglion cell line, F-11. *Dev. Brain Res.* **51**, 259–266 (1990).
59. Fan, S., Shen, K., Scheideler, M. & Crain, S. F11 neuroblastoma × DRG neuron hybrid cells express inhibitory μ- and δ-opioid receptors which increase voltage-dependent K+ currents upon activation. *Brain Res.* **590**, 329–333 (1992).

60. Wieringa, P., Tonazzini, I., Micera, S. & Cecchini, M. Nanotopography induced contact guidance of the F11 cell line during neuronal differentiation: a neuronal model cell line for tissue scaffold development. *Nanotechnology* **23**, 275102 (2012).
61. Prucha, J. et al. Acute exposure to high-induction electromagnetic field affects activity of model peripheral sensory neurons. *J. Cell. Mol. Med.* https://doi.org/10.1111/jcmm.13423 (2017).
62. Nickalls, R. W. D. & Mapleson, W. W. Age-related iso-MAC charts for isoflurane, sevoflurane and desflurane in man. *Br. J. Anaesth.* **91**, 170–174 (2003).
63. Esper, T., Wehner, M., Meinecke, C.-D. & Rueffert, H. Blood/gas partition coefficients for isoflurane, sevoflurane, and desflurane in a clinically relevant patient population. *Anesth. Analg.* **120**, 45–50 (2015).
64. Baker, P. F., Hodgkin, A. L. & Ridgway, E. B. Depolarization and calcium entry in squid giant axons. *J. Physiol.* **218**, 709–755 (1971).
65. Kerr, R. et al. Optical imaging of calcium transients in neurons and pharyngeal muscle of C. elegans. *Neuron* **26**, 583–594 (2000).
66. Tank, D. W., Sugimori, M., Connor, J. A. & Llinás, R. R. Spatially resolved calcium dynamics of mammalian purkinje cells in cerebellar slice. *Science* **242**, 773–777 (1988).
67. Sabatini, B. L., Oertner, T. G. & Svoboda, K. The life cycle of Ca2+ ions in dendritic spines. *Neuron* **33**, 439–452 (2002).
68. Zhou, X., Belavek, K. J. & Miller, E. W. Origins of Ca $^{2+}$ imaging with fluorescent indicators. *Biochemistry* **60**, 3547–3554 (2021).
69. Huang, L. et al. Relationship between simultaneously recorded spiking activity and fluorescence signal in GCaMP6 transgenic mice. *eLife* **10**, e51675 (2021).
70. Antonovaite, N., van Wageningen, T. A., Paardekam, E. J., van Dam, A.-M. & Iannuzzi, D. Dynamic indentation reveals differential viscoelastic properties of white matter versus gray matter-derived astrocytes upon treatment with lipopolysaccharide. *J. Mech. Behav. Biomed. Mater.* **109**, 103783 (2020).
71. Gruca, G., de Man, S., Slaman, M., Rector, J. H. & Iannuzzi, D. Ferrule-top micromachined devices: design, fabrication, performance. *Meas. Sci. Technol.* **21**, 094033 (2010).
72. Yin, S., Ruffin, P. B. & Yu, F. T. S. *Fiber Optic Sensors* (CRC press, 2008).
73. Rugar, D., Mamin, H. J. & Guethner, P. Improved fiber-optic interferometer for atomic force microscopy. *Appl. Phys. Lett.* **55**, 2588–2590 (1989).
74. Hine, R. & Inc Facts on File. *The Facts on File dictionary of biology. Facts on File Science Library* (Checkmark Books/Facts On File, New York, 2005), 4th ed edn.
75. Bartolini, L., Iannuzzi, D. & Mattei, G. Comparison of frequency and strain-rate domain mechanical characterization. *Sci. Rep.* **8**, 13697 (2018).
76. Van Hoorn, H., Kurniawan, N. A., Koenderink Ac, G. H. & Iannuzzi, D. Local dynamic mechanical analysis for heterogeneous soft matter using ferrule-top indentation. *Soft Matter* **12**, 3066 (2016).

Acknowledgements

This research was funded in whole, or in part, by the UKRI EPSRC Healthcare Technologies Challenge Award EP/N020987/1. For the purpose of Open Access, the author has applied a CC BY public copyright licence to any Author Accepted Manuscript version arising from this submission. Additionally, the authors acknowledge James Fisk for machining the airtight box to contain the isoflurane and Risto Martin for his assistance with the syringe pump, vaporiser and compressed air noise damping table. The authors also acknowledge Dr. Jacob Seifert and Zuzana Coculova for their insight on the loss tangent.

Author contributions

C.A., C.K., A.E. and A.J. designed the experiments. C.K. and A.E. designed the isoflurane delivery system used in the experiments. C.A. and C.K. performed the experimental measurements. C.K. collected and processed the majority of the DMA data. C.A. collected and processed the majority of the calcium imaging data. C.A. coded the data analysis scripts and analysed the data. C.A., S.C. and A.J. interpreted the data. H.Y. supervised the experimental work. A.J. supervised the overall work.

Competing interests

The authors declare no competing interests.

Additional information

Supplementary information The online version contains supplementary material available at https://doi.org/10.1038/s42005-023-01252-7.

Correspondence and requests for materials should be addressed to Casey Adam, Sonia Contera or Antoine Jerusalem.

Peer review information *Communications Physics* thanks Shivprasad Patil and the other, anonymous, reviewers for their contribution to the peer review of this work.

Reprints and permission information is available at http://www.nature.com/reprints

Publisher's note Springer Nature remains neutral with regard to jurisdictional claims in published maps and institutional affiliations.